J. Astrophys. Astr. (2011) **32,** 567–576 © Indian Academy of Sciences

The Large Scale Structure: Polarization Aspects

R. F. Pizzo
ASTRON, Postbus 2, 7990 AA Dwingeloo, The Netherlands
e-mail: pizzo@astron.nl

Abstract. Polarized radio emission is detected at various scales in the Universe. In this document, I will briefly review our knowledge on polarized radio sources in galaxy clusters and at their outskirts, emphasizing the crucial information provided by the polarized signal on the origin and evolution of such sources. Successively, I will focus on Abell 2255, which is known in the literature as the first cluster for which filamentary polarized emission associated with the radio halo has been detected. By using RM synthesis on our multi-wavelength WSRT observations, we studied the 3-dimensional geometry of the cluster, unveiling the nature of the polarized filaments at the borders of the central radio halo. Our analysis points out that these structures are relics lying at large distance from the cluster center.

Key words. Galaxies: clusters: general—galaxies: clusters: individual (Abell 2255)—galaxies: intergalactic medium—magnetic fields—polarization.

1. Introduction

In the hierarchical scenario of structure formation in the Universe, galaxy clusters are located at the nodes of the filamentary large-scale structure of the cosmic web and form by subsequent merging of smaller structures and the inflow of matter along the supercluster filaments (e.g. Evrard & Gioia 2002). Merger events drive shock waves and turbulence in cluster environments. These phenomena (re-) accelerate the relativistic particles of the intracluster medium (ICM), which, by interacting with the cluster magnetic field, give rise to extended diffuse synchrotron features named radio halos and relics, on the basis of their morphology, location within the cluster, and polarization properties.

Radio halos lie at the cluster center and are characterized by a typical size of $\sim$1 Mpc, a smooth roundish shape, low radio surface brightness ($\sim 10^{-6}$ Jy arcsec^{-2} at 1.4 GHz), steep radio spectrum ($\alpha \leq -1$, $S_\nu \propto \nu^\alpha$), and lack of any strong linear polarization (upper limit $\sim$10%). Relics are located at cluster peripheries; they exhibit a higher surface brightness than halos, but also have steep spectra. Their morphologies are irregular and often they are highly polarized (up to 50%). The low radio surface brightness and steep synchrotron spectrum make the detection of halos and relics rather difficult. In the past few years, however, several works on such sources

and their hosting clusters have improved our knowledge of their origin and physical properties (for reviews, see e.g. Giovannini *et al.* 2009; Ferrari *et al.* 2008). Possible formation scenarios have been proposed and are summarized in the following. Halo models can be grouped in two main classes: (i) *primary models*, where electrons undergo *in-situ* acceleration by turbulent gas motion or by shocks (e.g. Brunetti *et al.* 2001), (ii) *secondary models*, where the particles are produced by hadronic interaction of relativistic protons with the background gas of the ICM (e.g. Dennison 1980). On the other hand, radio relics have been suggested to be tracers of shock waves, which could directly accelerate the relativistic particles (Enßlin *et al.* 1998) or re-energize them by adiabatic compression, while confined in possible patches of fossil radio plasma (Enßlin & Gopal Krishna 2001). Internal Faraday rotation and/or beam depolarization (Burn 1966) could justify the absence of polarization in radio halos. Instead, the shock-related origin of radio relics directly explains their high level of polarization.

Together with these 'cluster related' sources, extended diffuse radio features have also been found at very large distance from cluster centers. A few examples are reported in the literature; see e.g. (i) the case of Abell 2255, for which two relic sources have been detected at a projected distance of 2 Mpc from the cluster center (Pizzo *et al.* 2008), (ii) the source 0917+75 detected at 3.8 Mpc from the nearest rich cluster (e.g Dewdney *et al.* 1991), (iii) the relic source in A2069 (Giovannini *et al.* 1999) at 4.6 Mpc from the cluster center, and (iv) the extended diffuse radio emission coincident with the filament of galaxies ZwCl2341.1+0000, 2.5 Mpc in size (Bagchi *et al.* 2002). These detections clearly show that particle acceleration and magnetic fields are ubiquitous in the Universe.

Important information on the nature and the properties of halos, relics, and filaments can be derived by studying their total intensity emission. Complementary crucial information on their origin, location, internal and external physics come from the study of their polarization. This is because the radio signal emitted by a radio source suffers Faraday rotation along the line-of-sight while crossing a magnetized and ionized plasma according to:

$$\chi_{\rm obs}(\lambda) = \chi_{\rm int} + \lambda^2 \times {\rm RM}, \tag{1}$$

where $\chi_{\rm int}$ is the intrinsic polarization angle of the signal, $\chi_{\rm obs}$ is the polarization angle observed at a wavelength λ, and RM is the plasma Rotation Measure.

The RM depends on the plasma magnetic field ($B_\parallel$) and electron density ($n_{\rm e}$) along the line-of-sight through

$${\rm RM\ [rad\ m^{-2}]} = 812 \int_0^{L_{\rm [kpc]}} n_{\rm e\ [cm^{-3}]} B_{\parallel [\mu{\rm G}]} {\rm dl}, \tag{2}$$

where L is the distance of the source from the observer. Note that the quantity expressed in equation (2) is generally referred to as Faraday depth (Φ) in the case that the emitting and Faraday rotating plasmas are not separated along the line-of-sight.

Several studies in the literature have shown that polarized emission is common to radio galaxies (e.g. Govoni *et al.* 2006), relics (see the example of galaxy cluster CIZA 2242, van Weeren *et al.* 2010) and filaments (e.g. ZwCl2341.1+0000, Giovannini *et al.* 2010). A useful tool to analyze and interpret polarimetric data is RM synthesis (Brentjens & de Bruyn 2005). The essence of this technique is that,

starting from the Q and U channel maps of the target field, it produces the so-called RM cube, which displays the polarized emission in the field of the target as a function of Faraday depth. By doing so, RM synthesis can give important information on the 3-dimensional structure of galaxy clusters, helping us in understanding the nature of the polarized features belonging to it.

2. The case of Abell 2255

A remarkable galaxy cluster hosting significant polarized emission is Abell 2255. This nearby ($z = 0.0806$, Struble & Rood 1999) and rich system has been studied at several wavelengths. In the radio domain, it hosts a diffuse radio halo, a relic source, and seven extended head–tail radio galaxies. On the basis of their morphology at low frequency, they have been named Goldfish, Double, Original TRG, Sidekick, Bean, Beaver, and Embryo (Harris *et al.* 1980). The first four lie near the cluster center, while the other three are located at a large projected distance from it ($\geq$2 Mpc). A study of the cluster at 21 cm through VLA observations revealed that the radio halo is dominated at the borders by 3 filaments that are strongly polarized ($\sim$20–40%, Govoni *et al.* 2005). In the literature, this represents the first detection of polarized radio emission from a radio halo. A few years after this discovery, polarized emission was also detected in the halo of the galaxy cluster MACS J0717.5 +3745 (Bonafede *et al.* 2009). The polarized signal ($\sim$17% at 4.8 GHz) in this case also is confined within a filament, which the data show to be connected to the central radio halo.

To understand the nature of the polarized filamentary signal in A2255, we observed the cluster with the Westerbok Synthesis Radio Telescope (WSRT) for a total of 300 hours at 18, 21, 25, 85 and 200 cm. The cluster is located at RA = $17^{\rm h}12^{\rm m}31^{\rm s}$, DEC = $+64^{\rm d}05^{\rm m}33^{\rm s}$ and has galactic co-ordinates $l = 94°$, $b = 35°$.

2.1 *Polarization imaging and RM cubes*

After calibration, we produced Q and U channel images for each dataset and we inspected them to remove those affected by residual RFI and/or problems related to specific telescopes. The final images were carried through for further processing in RM synthesis. To improve the resolution in RM space, as well as the sensitivity, we combined the 18, 21 and 25 cm datasets, producing a single high-frequency RM cube. In addition, we made RM cubes at 85 and 200 cm. In the following sections, I will present and discuss the properties of the high-frequency and 85-cm RM cubes.

2.1.1 *RM cube at 18+21+25 cm.* The high-frequency RM cube[1] covers a field of view of 1.5° × 1.5° and samples a range of Faraday depths from -1000 to $+1000$ rad m^{-2}, with a step of 10 rad m^{-2}. To increase the signal-to-noise ratio for the extended low brightness structures, we made an RM-cube at half spatial resolution (FWHM = $28'' \times 30''$). This has a noise of approximately 10 μJy beam^{-1}.

[1] A2255_18_21_25CM.gif, only available in electronic form at the CDS via anonymous ftp to cdsarc.u-strasbg.fr (130.79.128.5) or via http://cdsweb.u-strasbg.fr/cgi-bin/qcat?J/A+A/

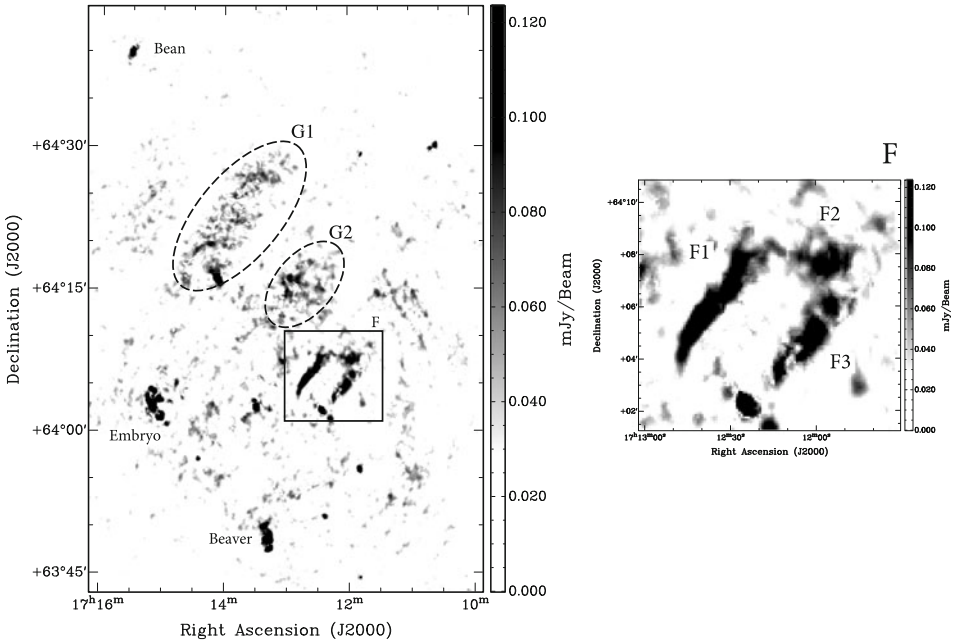

Figure 1. *Left panel*: Polarized intensity (in units of mJy beam^{-1} RMSF^{-1}) in the field of A2255 from the high-frequency RM cube (18 cm + 21 cm + 25 cm) at $\phi = +30$ rad m^{-2}. *Right panel*: Zoom into the region where the radio filaments are located.

As an example of the astronomical signal detected in the field of A2255 in this cube, in Fig. 1 we show the frame at $\phi = +30$ rad m^{-2}. We can distinguish two main polarized components:

- the first is associated with the cluster sources, i.e. radio galaxies and filaments. This component extends between -200 and $+200$ rad m^{-2}, with each structure covering its own range of Faraday depths;
- the second is associated to two large-scale polarized structures (labeled G1 and G2 in Fig. 1). That these components have no counterpart in total intensity favors an association with the galactic foreground (e.g. Wieringa *et al.* 1993). They appear at Faraday depths between -20 rad m^{-2} and $+80$ rad m^{-2} and peak at $\phi \sim 30$ rad m^{-2}.

2.1.2 *RM cube at 85 cm.* This RM cube[2] covers a field of view of $6° \times 6°$ and synthesizes a range of Faraday depths from -400 to $+400$ rad m^{-2}, with a step of 4 rad m^{-2}. Its rms noise is 45 μJy beam^{-1} (FWHM $= 54'' \times 64''$), the lowest achieved at such a long wavelength to date.

The RM cube shows bright polarized emission with an astronomical origin. This is mostly detected in the RM range -20 rad m$^{-2} \leq \phi \leq +50$ rad m^{-2} and is likely

[2]A2255_85CM.gif, only available in electronic form at the CDS via anonymous ftp to cdsarc.u-strasbg.fr (130.79.128.5) or via http://cdsweb.u-strasbg.fr/cgi-bin/qcat?J/A+A/

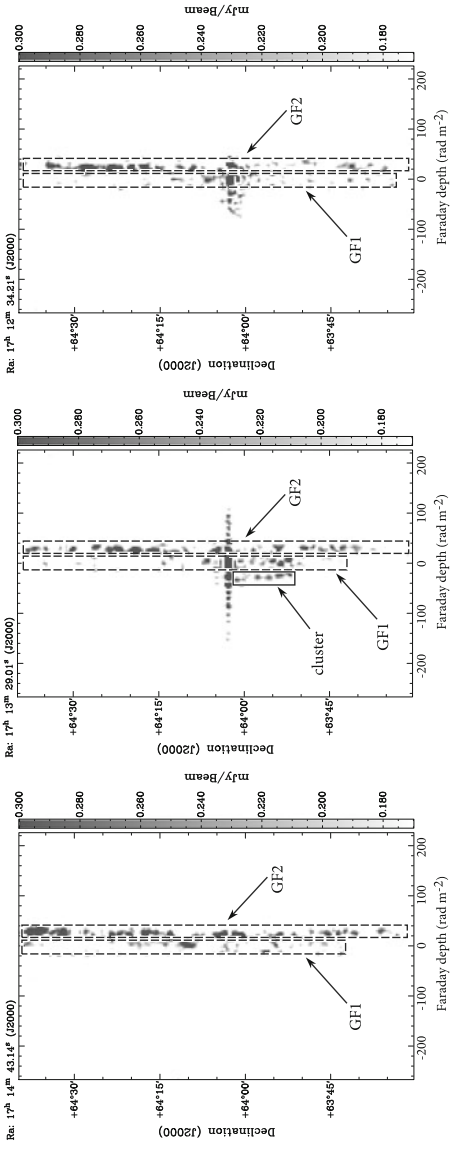

Figure 2. The polarized emission in the 85-cm RM cube in units of mJy beam^{-1} RMSF^{-1}. From left to right, the situation at decreasing values of right ascension is presented. The right ascension value is reported in the upper left corner of each panel. At RA = $17^{\rm h}13^{\rm m}29^{\rm s}$ three polarized components are detected, nominally the cluster emission ("cluster") and the two Galactic Faraday screens (GF1 and GF2). These two components are the only ones detected at the other right ascensions. The emission at location DEC = $+64°02'43''$ and extending in Faraday depth between -70 rad m^{-2} to $+100$ rad m^{-2} comes from the double radio galaxy.

associated with our Galaxy, since it extends well beyond the cluster 'boundary' and it has no counterpart in total intensity. In addition, the cube shows also features that suggest an association with continuum structures belonging to A2255. This emission focuses in the southern regions of the cluster and between declinations $+63°51' 48''$ and $+63°59' 33''$. To show this, we produced images of the polarized emission at the location of the cluster as a function of RA (see Fig. 2). The central panel of Fig. 2 refers to RA $= 1^{h}13^{m}29^{s}$. Here we can distinguish 3 components of polarized emission in the field. Two of them are located at $\phi \sim 0$ rad m^{-2} and at positive Faraday depths (GF1 and GF2) and represent the two screens due to our Galaxy. The last one is visible at Faraday depths ranging between -32 rad m^{-2} and -16 rad m^{-2} and is only detected at this specific value of right ascension. This is confirmed by the left and the right panels of Fig. 2, where the situation at RA to the east and to the west of the cluster is presented.

By inspecting the original RM cube at the Faraday depths at which the cluster component is detected here, we note that this is associated with the tail of the Beaver radio galaxy (see Fig. 10 in Pizzo *et al.* 2011), which is undetected in total intensity and polarization at higher frequencies.

2.2 *Rotation measure structure*

To investigate the location of the radio galaxies and of the filaments within the cluster, we extracted their Faraday spectra from the high-frequency RM cube and we also computed their RM images. The Faraday spectra of the radio galaxies have various levels of complexity (see Fig. 11 in Pizzo *et al.* 2011). The sources that lie in projection near the cluster center (Double, TRG and Goldfish) have Faraday spectra characterized by one main peak at a specific Faraday depth, plus significant secondary peaks (above 5σ) at different Faraday depths. This property reflects on the complexity of the RM distributions of the same radio galaxies, which are characterized by a complex and non-Gaussian profile. On the other hand, the radio galaxies which lie at large projected distance from the cluster center (Bean, Embryo and Beaver, see Fig. 11 in Pizzo *et al.* 2011) and the radio filaments (see Fig. 13 in Pizzo *et al.* 2011) show Faraday spectra with only one significant peak. Table 1 lists the mean $\langle \mathrm{RM} \rangle$ value, the σ_{RM}, and the maximum absolute value of the RM distributions of these sources. It is clear that the external radio galaxies and the filaments have similar $\langle \mathrm{RM} \rangle$ and σ_{RM} values ($\langle RM \rangle \sim +20$ rad m^{-2}, $\sigma_{\mathrm{RM}} \sim 10$ rad m^{-2}).

Table 1. Parameters of the RM-distributions for the external radio galaxies and for the filaments.

Name	$\lvert \mathrm{RM_{max}} \rvert$ (rad m^{-2})	$\langle \mathrm{RM} \rangle$ (rad m^{-2})	σ_{RM} (rad m^{-2})	Dist (r/r_{c})
F1	52	24	9	0.7
F2	47	14	13	1.2
F3	70	25	15	1.5
Embryo	47	25	9	3.1
Beaver	74	37	13	4.1
Bean	40	19	11	7.5

3. Discussion

3.1 *The radio galaxies*

The RM distribution of cluster radio sources carries important information on the magneto-ionic properties (electron density and magnetic field along the line-of-sight) of the external medium. If, in the simplest case, this is characterized by a magnetic field that is tangled within cells of uniform size and it has the same strength and random orientation within them, the observed RM along any given line of sight is represented by a random walk process. Therefore, the distribution of RM results in a Gaussian with zero mean and the dispersion is related to the number of cells along the line-of-sight.

Several studies of the RM distribution of extended radio galaxies in clusters have pointed out that there is a significant trend between the observed RM distribution and the projected distance of the source from the cluster center (e.g. Feretti *et al.* 1999): the smaller the projected distance from the core, the higher $\sigma_{\rm RM}$ and $\langle {\rm RM} \rangle$. This result suggests that the external Faraday screen for all the cluster sources is the ICM of the cluster, which modifies the polarized radio signal depending on how much magneto-ionized medium it crosses[3].

The polarimetric properties of three radio galaxies belonging to A2255 (the Double, the Original TRG and the Beaver) have been studied by Govoni *et al.* (2006) by means of high-frequency (1.4 GHz) VLA observations of the cluster. The central sources (the original TRG and the Double) show the highest $\sigma_{\rm RM}$ and $\langle {\rm RM} \rangle$ of the sample, while the peripheral radio galaxy (the Beaver) shows a low value of $\langle {\rm RM} \rangle$ ($= +36$ rad m^{-2}) and a comparable dispersion ($\sigma_{\rm RM} = 42$ rad m^{-2}). Our data confirm the result for the Beaver and extend the analysis to the other peripheral radio galaxies (Embryo and Bean), which also show small $\langle {\rm RM} \rangle$ and $\sigma_{\rm RM}$. By combining our results with those of Govoni *et al.* (2006), it is evident that in the case of A2255 also, the external screen for the radio galaxies is the ICM. This affects not only the RM distribution of the cluster radio galaxies, but also the complexity of their Faraday spectra. Radio galaxies at different projected distances from the cluster center show Faraday spectra with different levels of complexity. The sources in the outermost cluster regions (Bean, Beaver and Embryo) have simple spectra, mainly showing one peak, while the radio galaxies located in the central areas of the cluster have complex Faraday spectra, showing multiple peaks. Since the co-location along the line-of-sight of multiple emitting and rotating regions produces Faraday spectra with multiple peaks (Brentjens & de Bruyn 2005), we conclude that the radio galaxies showing the most complex spectra (and accordingly the broadest RM distributions) are likely to be located deep inside the ICM or behind the cluster. On the other hand, the radio galaxies showing the less complex spectra (and the smallest RM distributions) is likely to lie in the external regions of the ICM. These results

[3]It is worth noting that the RM observed towards cluster radio galaxies may not be entirely representative of the cluster magnetic field if the RM is locally enhanced by the compression of the ICM from the motion of the source through it. However, this hypothesis is ruled out because Clarke *et al.* (2004) showed that the RM distribution of point sources seen at different impact parameters from the cluster center has a broadening towards the center of the cluster. This result reveals that most of the RM contribution comes from the ICM.

show that the RM distributions and the Faraday spectra of cluster radio galaxies help in revealing their 3-dimensional location within the cluster.

3.2 *The Beaver radio galaxy*

In the 85-cm RM cube, the tail of the Beaver radio galaxy is detected between -32 rad m$^{-2} < \phi <$–16 rad m^{-2}. On the other hand, the head and the initial part of the tail of the source are detected in the high-frequency RM cube at a Faraday depth of $\sim +37$ rad m^{-2}, at which, in the 85-cm RM cube, the emission mainly comes from the galactic foreground. The RM gradient between head and tail can give strong constraints on the possible location of these two structures within A2255. It is worth noting that the head and the initial part of the tail show RM values that are similar to those of the galactic foreground at the location of A2255 (Pizzo *et al.* 2011). This suggests that the head of the Beaver is located at the outskirts of the cluster and, in particular, in the foreground of A2255, where only a small portion of ICM is crossed by the radio signal before reaching the observer. That the tail appears at negative Faraday depths instead implies that it should be located deeper in the ICM. Therefore, the Beaver could not lie in the plane of the sky, but with the tail pointing towards the central radio halo, possibly connecting with it[4]. This interpretation is supported by the common spectral index values found for the end of the tail and the southern region of the halo (Pizzo & de Bruyn 2009). The sketch in Fig. 3 illustrates this situation.

3.3 *The filaments*

Our polarimetric data confirm the strong polarization of the filaments found by Govoni *et al.* (2005) and add an important information that help explain their nature. The filaments have polarimetric properties similar to those found for the external radio galaxies of A2255, i.e. the Embryo, the Beaver and the Bean. Their RM distributions are characterized by low values of $\sigma_{\rm RM}$ and $\langle {\rm RM} \rangle$, and their Faraday spectra show only one peak. Following the interpretation given for the radio galaxies (see §3.1), these results suggest that the filaments are not located deep in the ICM, but at the periphery of the cluster. Moreover, given their high fractional polarization and their small spatial RM variance, we conclude that they should be located in the foreground of the cluster and not in the background. Since the RM distribution and the complexity of the spectra of the galactic regions G1 and G2 (see Fig. 1) are similar to that of the filaments (Pizzo *et al.* 2011), we conclude that most of the contribution to the Faraday depth of the filaments comes from our Galaxy and suggests that the they should lie at large distance from the cluster center[5]. The observed central

[4]The Faraday spectrum of the tail of the Beaver shows multiple secondary peaks, favoring a location of this part of the source deep in the ICM. However, it is worth noting that such a complexity could partly be due to the galactic foreground, which dominates the field at the location of this source at more positive Faraday depths.

[5]For comparison, see the case of the relic of A2256, for which an uniform RM and low RM dispersion have been found, indicating that this source lies in the foreground of the cluster, where the RM contribution of the ICM is small.

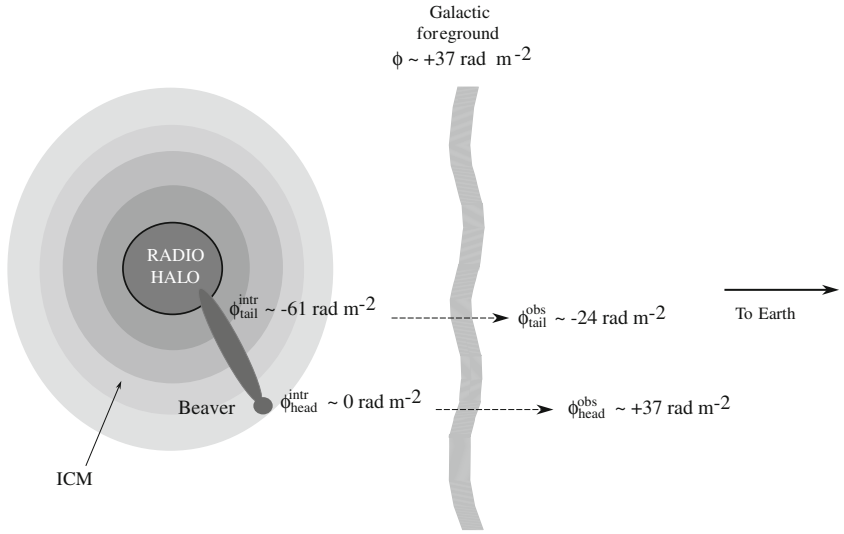

Figure 3. Possible 3-dimensional location of the Beaver radio galaxy within A2255. The grey-scale for the ICM represents an increasing electron density of the plasma towards the cluster center. Our Galaxy contributes to the observed Faraday depths ($\phi^{\rm obs}_{\rm head}$ and $\phi^{\rm obs}_{\rm tail}$) at which the head and the tail appear in the RM cubes.

location of the filaments, therefore, should be considered as due to a projection effect. *On the basis of the elongated shape and the high degree of linear polarization of the filaments, we therefore argue that they are relics rather than part of a genuine radio halo*. That the halo and the filaments of A2255 could be two unrelated features is also suggested by the halo spectral index distribution (Pizzo & de Bruyn 2009), showing an uncommon radial flattening with increasing distance from the center. Such a result also clearly indicates that fresh particle acceleration, likely due to shocks, takes place along the filaments. Evidence for shocks at this location should be supported by good resolution X-ray observations. Such data, hopefully available in the near future, are also important to understand at which distance from the cluster center these features are located and in particular whether they are confined within the cluster environment or associated with the cosmic web.

Acknowledgements

The Westerbork Synthesis Radio Telescope is operated by ASTRON (Netherlands Institute for Radio Astronomy) with support from the Netherlands Foundation for Scientific Research (NWO).

References

Bagchi, J., Enßlin, T. A., Miniati, F. *et al.* 2002, *New Astron.*, **7**, 249.
Bonafede, A., Feretti, L., Giovannini, G. *et al.* 2009, *Astron. Astrophys.*, **503**, 707.
Brentjens, M. A., de Bruyn, A. G. 2005, *Astron. Astrophys.*, **441**, 1217.
Brunetti, G., Setti, G., Feretti, L., *et al.* 2001, *Mon. Not. R. Astron. Soc.*, **320**, 365.

Burn, B. J. 1966, *Mon. Not. R. Astron. Soc.*, **133**, 67.
Clarke, T. E. 2004, *J. Korean Astron. Soc.*, **37**, 337.
Dennison, B. 1980, *Astrophys. J. Lett.*, **239**, L93.
Dewdney, P. E., Constain, C. H., McHardy, I. *et al.* 1991, *Astrophys. J. Suppl.*, **76**, 1055.
Enßlin, T. A., Biermann, P. L., Klein, U. *et al.* 1998, *Astron. Astrophys.*, **332**, 395.
Enßlin, T. A., Gopal-Krishna 2001, *Astron. Astrophys.*, **366**, 26.
Evrard, A. E., Gioia, I. M. 2002, in Astrophysics and Space Science Library, Vol. 272, Merging Processes in Galaxy Clusters, ed. L. Feretti, I. M. Gioia, & G. Giovannini, pp. 253–304.
Feretti, L., Dallacasa, D., Govoni, F. *et al.* 1999, *Astron. Astrophys.*, **344**, 472.
Ferrari, C., Govoni, F., Schindler, S. *et al.* 2008, *Space Sci. Rev.*, **134**, 93.
Giovannini, G., Tordi, M., Feretti, L. 1999, *New Astron.*, **4**, 141.
Giovannini, G., Bonafede, A., Feretti, L. *et al.* 2009, *Astron. Astrophys.*, **507**, 1257.
Giovannini, G., Bonafede, A., Feretti, L. *et al.* 2010, *Astron. Astrophys.*, **511**, L5.
Govoni, F., Murgia, M., Feretti, L. *et al.* 2005, *Astron. Astrophys.*, **430**, L5.
Govoni, F., Murgia, M., Feretti, L. *et al.* 2006, *Astron. Astrophys.*, **460**, 425.
Harris, D. E., Kapahi, V. K., Ekers, R. D. 1980, *Astron. Astrophys. Suppl.*, **39**, 215.
Pizzo, R. F., de Bruyn, A. G. 2009, *Astron. Astrophys.*, **507**, 639.
Pizzo, R. F., de Bruyn, A. G., Bernardi, G. *et al.* 2011, *Astron. Astrophys.*, **525**, A104+.
Pizzo, R. F., de Bruyn, A. G., Feretti, L., Govoni, F. 2008, *Astron. Astrophys.*, **481**, L91.
Struble, M. F., Rood, H. J. 1999, *Astrophys. J. Suppl.*, **125**, 35.
van Weeren, R. J., Röttgering, H. J. A., Brüggen, M. *et al.* 2010, *Science*, **330**, 347.
Wieringa, M. H., de Bruyn, A. G., Jansen, D. *et al.* 1993, *Astron. Astrophys.*, **268**, 215.